

## Power Flow Control in the Converters Interconnecting AC-DC Meshed Systems

**Abstract.** DC grids are being strongly considered as a technology to be used for future expansions of the transmission system. Voltage sourced converters (VSC) are the key equipment considered for AC/DC interconnections. However the flow from DC to AC system has to be properly set as many alternatives exists. In this article, an Optimal Power Flow (OPF) to control the flow of power in the converters interconnecting AC-DC systems is presented. The proposed OPF solution technique was tested using the CIGRE B4 DC Grid Test System.

**Streszczenie.** W artykule opisano sterowanie przepływem mocy w przekształtniku łączącym sieci DC-AC. Optymalny przepływ mocy OPF był testowany w systemie sieciowym CIGRE B4 DC. **Sterowanie przepływem mocy w przekształtniku łączącym sieci DC-AC**

**Keywords:** AC-DC Grid, Optimal Power Flow, Power Flow Control, VSC Converters.

**Słowa kluczowe:** sieć AC-DC, sterowanie przepływem mocy

### Introduction

A DC grid overlapping the existing ac grid is being considered for future expansions of the European electrical system [1]. This dc grid will integrate offshore wind farms and photovoltaic generation interconnecting several countries.

This technology may also be used in others countries. One important characteristic is that it will include the VSC technology, underground/submarine cables as well as overhead transmission lines.

As a new feature new tools and procedures have to be developed similarly to the ac grid technology [2, 3].

VSC converters have the inherent capability to control: active power or DC voltage (by acting in the angle of its generated voltage) and the AC voltage or reactive power (by acting in the magnitude of the generated voltage). This offers a robust control of the power flow in the system [4].

To develop a power flow study, the existing tools have to be modified by inserting these new concepts [5, 6, 7].

The integrated AC/DC system shown in Fig. 1 was considered by the SC-B4 of CIGRE [8].

In Fig. 1, onshore AC busses are called “Ba”, offshore AC busses “Bo”, sym. monopole DC busses “Bm”, bipole DC busses “Bb”, monopole AC-DC converter stations “Cm”, bipole AC-DC converter stations “Cb” and DC-DC converter stations “Cd”.

The system has a 380 kV AC grid interconnected to a 400/200 kV DC grid. The loads are located mainly in the AC system whereas the generation in the DC grid. To run the power flow of this integrated system two swing buses are considered (Ba-B0 and Ba-A0). Bus Bm-B2 is a voltage controlled bus to helps emergencies in the 200 kV subsystems. The active powers are set in the generations and DC loads (converters). Also, for the converters located in the interconnections (Bb-B1, Bb-B2 and Bm-B3) the active power must be an input, this introduces a degree of freedom thus many alternatives (with the same total MW) may be established.

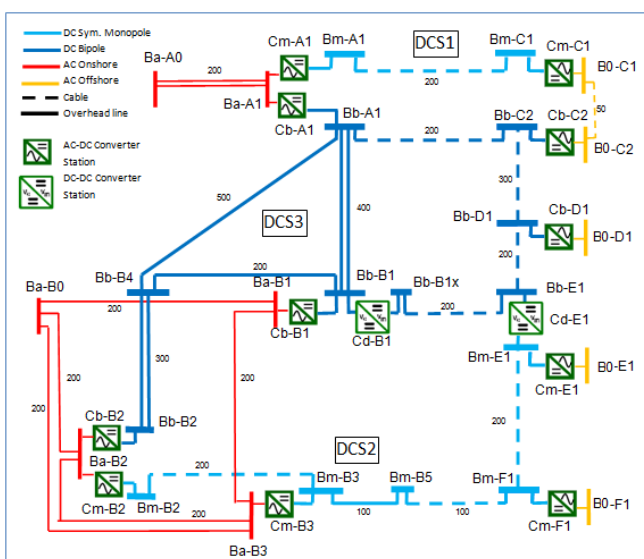
In Fig. 1, buses Bm-A1, Bm-C1 and also Bm-E1, Bm-F1, Bm-B5, Bm-B3, Bm-B2 are 200 kV systems and symmetrical monopolar converters.

Optimal power flow (OPF) is commonly used in AC system studies [9] of some countries. However, this cannot be the case of other countries where there is no active power flow control in the AC system and the voltage or reactive power control is not of primary concern.

Still, to study AC/DC interconnected systems this optimal power flow concept should be a necessary technique to be inserted as there is a freedom to set the converter power in the main interconnection (Cb-B1, Cb-B2 and Cm-B3). In this paper, an optimal power flow solution to control the power flow in the interconnections of the AC-DC systems is presented. In order to show the accuracy as well as the efficiency of the proposed solution technique, the proposed OPF was tested in the CIGRE B4 DC Grid Test System. This is the main goal of this paper whose structure is as follows. Section Two describes the load flow model. The OPF equations are established in Section Three. Section Four shows the results of the study case (Fig. 1). Finally, Section Five presents the main conclusions of the study.

### Mathematical Modeling

In this section, the mathematical modeling to analyze the AC/DC power flow, including those in the VSC converters, is presented.



### AC model

In order to model the steady state operating point of an AC system, the conventional equations of the AC power flow, shown in [9], can be used.

$$(1) \quad P_k^G - P_k^D - V_k \sum_{m \in \Omega} V_m (G_{km} \cos(\theta_{km}) + B_{km} \sin(\theta_{km})) = 0$$

$$(2) \quad Q_k^G - Q_k^D - V_k \sum_{m \in \Omega} V_m (G_{km} \sin(\theta_{km}) - B_{km} \cos(\theta_{km})) = 0$$

In (1) and (2),  $\Omega$  represents the number of buses within the AC system. The approach considers a reference bus and PQ type buses.  $P_k^G$  and  $P_k^D$  are the generation and load active power at bus  $k$ , respectively.  $Q_k^G$  and  $Q_k^D$  represent the reactive power at bus  $k$ , respectively.  $V_k$  is the voltage magnitude at bus  $k$ .  $\theta_{km} = \theta_k - \theta_m$  represents the phase angle difference between  $k$  and  $m$  buses.  $G_{km}$  and  $B_{km}$  represent the  $(k, m)$  elements of the  $Y_{bus}$  matrix (real and imaginary parts, respectively). The losses in the ac system can be obtained through (3).

$$(3) \quad \sum_{km \in \Omega_i} g_{km} (a_{km}^2 V_k^2 + V_m^2 - 2a_{km} V_k V_m \cos(\theta_{km}))$$

where,  $\Omega_i$  is the number of branches in the AC system. The term  $a_{km}$  represents the transformer voltage ratio whereas  $g_{km}$  is the conductance of each branch.

### DC Model

The power balance equation for the system depicted in Fig. 2 is given by (4).

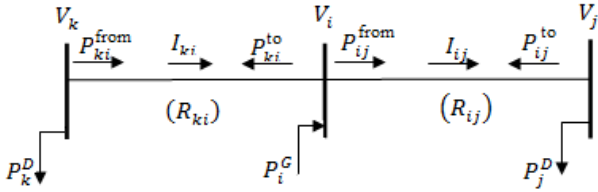


Fig. 2. Illustrative section of the dc system

$$(4) \quad P_i^G - P_i^D - \sum_{ki \in \Omega_i^{cc}} P_{ki}^{to} - \sum_{ij \in \Omega_i^{cc}} P_{ij}^{from} = 0$$

where,  $\Omega_i^{cc}$  and  $\Omega_i^{cc}$  represent the number of buses and branches within the dc system, respectively.

The active power flow  $P_{ij}^{from}$  and  $P_{ki}^{to}$ , as well as the magnitude of the current ( $I_{ij}$ ) in the  $i, j$  branch, are given by (5) and (6), respectively.

$$(5) \quad \left. \begin{aligned} P_{ij}^{from} &= V_i \frac{(V_i - V_j)}{R_{ij}} \quad (a) \\ P_{ij}^{to} &= V_j \frac{(V_j - V_i)}{R_{ij}} \quad (b) \end{aligned} \right\}$$

$$(6) \quad I_{ij} = \frac{V_i - V_j}{R_{ij}}$$

$R_{ij}$  is the circuit resistance within the  $(i, j)$  segment.  $P_{ij}^{from}$  and  $P_{ij}^{to}$  are the active power flow from bus  $i$  to bus  $j$  and from bus  $j$  to bus  $i$ , respectively.

The steady state operating point of a DC system can be represented by (4)-(6). Another equivalent representation of (5) can be (7).

$$(7) \quad \left. \begin{aligned} P_{ij}^{from} + P_{ij}^{to} &= R_{ij} I_{ij}^2 \quad (a) \\ P_{ij}^{from} - P_{ij}^{to} &= \frac{1}{R_{ij}} (V_i^2 - V_j^2) \quad (b) \end{aligned} \right\}$$

The losses in the  $(i, j)$  segment can be determined through (7). In this case, expressions (5a) and (5b) are replaced by (7a) and (7b), respectively. Thus, (4), (6) and (7) are used to represent the steady state operation of the dc system. The losses in the DC system can be obtained through (8).

$$(8) \quad \sum_{ij \in \Omega_i^{cc}} R_{ij} I_{ij}^2$$

### Converter model

The equivalent model of the AC-DC converter is shown in Fig. 3. It can be seen that the only variable coupling both AC and DC systems is the injected active power.

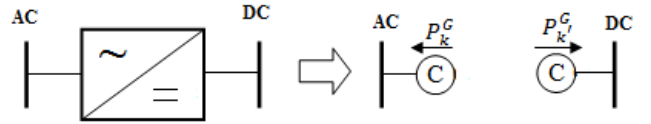


Fig. 3. VSC representation as equivalent sources

The converter coupling constraint is shown in (9). Note that the active losses in the AC-DC converters are represented by  $P_{AC-DC}^{Loss}$ . To this work  $P_{AC-DC}^{Loss}$  was considered equal as 1% per station [10].

$$(9) \quad P_k^G + P_{k'}^G + P_{AC-DC}^{Loss} = 0$$

Additionally, an equality restriction that fixes/determines the active power exchange between both AC-DC subsystems can be considered (10).

$$(10) \quad \sum_{\forall kk' \in \Omega_{cnv}} P_k^G = P_{cnv}^{total}$$

where  $\Omega_{cnv}$  represent the number of converters. In (10),

$P_{cnv}^{total}$  represents the total active power exchange between the whole AC and the whole DC system.

On the other hand, the DC-DC converter consists of an ideal DC-DC converter and 4 passive elements. The DC-DC converter is modeled as a current source on the Left-side and as a voltage source on the Right-side, Fig. 4 [8].

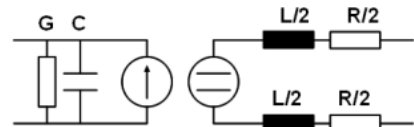


Fig. 4. Model of the DC-DC converter [8]

To this work DC-DC converter was represented by equivalent resistance.  $P_{DC-DC}^{Loss}$  was considered equal as 0.75% per station [11].

## Optimal Power Flow Modeling

The OPF objective is to minimize the total losses (active power) in both ac and dc systems.

Notice that the mathematical model presented in (11) is a nonlinear programming problem. This problem can be solved using commercially available tools (*solvers*) [12, 13, 14]. The objective function in (11) is represented by the total active losses in both AC-DC systems.

$$\begin{aligned}
 & \text{Min } \sum_{km \in \Omega_i} g_{km} (a_{km}^2 V_k^2 + V_m^2 - 2a_{km} V_k V_m \cos(\theta_{km})) + \sum_{ij \in \Omega_j^c} R_{ij} I_{ij}^2 \\
 & \text{Subject to:} \\
 & P_k^G - P_k^D - V_k \sum_{m \in \Omega} V_m (G_{km} \cos(\theta_{km}) + B_{km} \sin(\theta_{km})) = 0 \\
 & Q_k^G - Q_k^D - V_k \sum_{m \in \Omega} V_m (G_{km} \sin(\theta_{km}) - B_{km} \cos(\theta_{km})) = 0 \\
 & P_i^G - P_i^D - \sum_{ki \in \Omega_i^r} P_{ki}^{to} - \sum_{ij \in \Omega_j^c} P_{ij}^{from} = 0 \\
 & P_{ij}^{from} + P_{ij}^{to} = R_{ij} I_{ij}^2 \\
 & P_{ij}^{from} - P_{ij}^{to} = \frac{1}{R_{ij}} (V_i^2 - V_j^2) \\
 & I_{ij} = \frac{V_i - V_j}{R_{ij}} \\
 & P_k^G + P_k^G + P_{AC-DC}^{Loss} = 0 \\
 & \sum_{\forall kk \in \Omega_{cnv}} P_k^G = P_{cnv}^{total} \\
 & P_{cnv}^{total} \leq P_{cnv}^{max} \\
 & P_{ij}^{from}, P_{ij}^{to} \leq P_{ij}^{max}
 \end{aligned} \tag{11}$$

Some other operational restrictions can be added to the model presented in (11), namely: a) limitations to the voltage magnitude in both systems; b) impose limits to the apparent power in the ac system and; c) maximum limits to the active and reactive power generated.

As for the choice of the objective function, some other options like the transmission line congestion management or the transmission costs (when the transmission service is charged based on the power flow on the line) may also be proposed.

## Tests and Results

The model validation was done regarding the system depicted in Fig. 1. The input data of both AC and DC systems are those presented in Appendix.

The proposed model was implemented in the AMPL mathematical modeling language [12], and solved using the KNITRO commercial solver [14].

Next, the solutions obtained for different operating conditions are presented.

### Case 1 - Considering as a known variable the power exchange of the interconnection converters (Base Case)

This case assumes that the power exchange in the converters (Cb-B1, Cb-B2 and Cm-B3) is known. The respective values being:

$$\begin{aligned}
 \text{Cb-B1} &= 1500.0 \text{ MW} \\
 \text{Cb-B2} &= 1700.0 \text{ MW} \\
 \text{Cm-B3} &= 800.0 \text{ MW}
 \end{aligned}$$

The ranges of the voltages obtained are presented in Table 1.

It can be observed that regarding a 4000 MW power exchange of the converters, the total loss (active power) is equal to 40.76 (40.66 to DC system + 0.10 to AC system) MW.

For the system proposed, the AC system active power loss is very small due to the low impedances and low load considered in AC lines.

Note that Bm-B2 is voltage controlled bus therefore converter flow is not fixed (Cm-B2).

Table 1. Case 1- Voltage Solution

System	Voltage (p.u.)
Ba	1.032 to 1.050
Bm	0.985 to 0.996
Bb	0.992 to 1.001

### Case 2 - Regarding a free exchange between the systems

The ranges of the voltages obtained considering the minimization of the losses as well as the power exchange of the converters as optimization variables (with the only restriction that the sum of the exchanged power must be equal to 4000 MW) are presented in Table 2.

Table 2. Case 2- Voltage Solution

System	Voltage (p.u.)
Ba	1.032 to 1.050
Bm	0.980 to 0.990
Bb	0.990 to 1.000

In this case, the total active power loss is 39.96 (39.82 to DC system + 0.14 to AC system) MW. The sum of all the power exchanges is equal to 4000 MW. The optimal power exchange of the converters being:

$$\begin{aligned}
 \text{Cb-B1} &= 1550.44 \text{ MW} \\
 \text{Cb-B2} &= 1679.98 \text{ MW} \\
 \text{Cm-B3} &= 769.58 \text{ MW}
 \end{aligned}$$

Therefore, the optimization procedure is necessary to define the better value of the power injected.

### Case 3 - Considering the transmission limit in the DC cable Bb-B1-Bb-E1 (Congestion)

In Table 3, the ranges of the voltages obtained considering the criterion of minimizing the losses; the transmission limit at line Bb-B1-Bb-E1 (equal to 150 MW) and the power exchange of the converters as optimization variables (with the only restriction that the sum of the exchanged power must be equal to 4000 MW) are presented.

Table 3. Case 3- Voltage Solution

System	Voltage (p.u.)
Ba	1.032 to 1.050
Bm	0.985 to 0.996
Bb	0.992 to 1.001

In this case, the total active power loss is 40.42 (40.31 to DC system + 0.11 to AC system) MW. The sum of all the power exchanges is equal to 4000 MW. The power flow at line B1-E1 is equal to 150 MW. The optimal power exchange of the converters being:

$$\begin{aligned}
 \text{Cb-B1} &= 1518.84 \text{ MW} \\
 \text{Cb-B2} &= 1682.04 \text{ MW} \\
 \text{Cm-B3} &= 799.12 \text{ MW}
 \end{aligned}$$

## Conclusion

The dc grid with VSC converters has a good power exchange control capability. Therefore, an OPF tool should be required in order to orient the choice of the converter active power setting points in the interconnections.

The VSC in the ac/dc interconnection can control power or the dc voltages.

The proposed OPF was tested in the initial CIGRE B4 DC Grid Test System, illustrating how an interconnected AC-DC system should perform.

## REFERENCES

- [1] Available in: <http://www.friendsofthesupergrid.eu/>. Access date: July 12, (2013).
- [2] CIGRE Working Group B4-38, "Modeling and Simulation Studies to be performed during the lifecycle of HVDC Systems", (2013).

- [3] CIGRE Working Group B4-52, "HVDC Grid Feasibility Study", Electra, (2013).
- [4] CIGRE Working Group B4-37, "VSC Transmission", (2005).
- [5] J. Beerten, S. Cole and R. Belmans, "Generalized Steady-State VSC MTDC Model for Sequential AC/DC Power Flow Algorithms", *IEEE Transactions on Power Systems*, (2012), vol. 27, pp. 821-829.
- [6] Z. Xiao-Ping, "Multiterminal voltage-sourced converter-based HVDC models for power flow analysis", *IEEE Transactions on Power Delivery*, (2004), vol. 19, pp. 1877-1884.
- [7] M. A. B. Horita, J. A. Jardini, M. T. Bassini, G. Y. Saiki, M. R. Cavalheiro "Load Flow Calculation in a Hybrid AC and DC Grid", *Colloquium HVDC and Power Electronics to Boost Network Performance*, October 2-3, (2013), Brasilia - Brazil
- [8] T. K. Vrana, Y. Yang, D. Jovcic, S. Dennetière, J. A. Jardini, H. Saad "The CIGRE B4 DC Grid Test System", Electra, N. 270, October, (2013).
- [9] G.W. Stagg, A.H. El-Abiad, "Computer Methods in Power System Analysis", McGraw Hill, (1968).
- [10] Jacobson, B., Westman, B., Bahrman, M. P. "500 kV VSC Transmission System for Lines and Cables", 2012 San Francisco Colloquium. Advances in Voltage Source Converter Technologies, (2012).
- [11] Knight, M. "Offshore Grid Technology: Technology Options and Practical Issues for Offshore Networks", Cigré Workshop on Offshore Networks, (2011).
- [12] Fourer, R., Gay, D. M. e Kernighan, B. W. "AMPL: A modeling language for mathematical programming", CA: Brooks/Cole-Thomson Learning, Pacific Grove, (2003).
- [13] ILOG. "CPLEX Optimization subroutine library guide and reference", version 11.0, Incline Village, NV, USA, (2008).
- [14] R. H. Byrd, J. Nocedal, and R. A. Waltz, "KNITRO: An Integrated Package for Nonlinear Optimization" in *Large-Scale Nonlinear Optimization*, G. di Pillo and M. Roma, eds, pp. 35-59 (2006).

#### Appendix

The input data of both AC and DC systems are presented. Table 1 introduces the subsystem voltages. Table 2 introduces bus data.

Table 1. Subsystem Voltages

System	Voltage [kV]
AC Onshore	380
AC Offshore	145
DC Sym. Monopole	+/-200
DC Bipole	+/-400

Table 2. AC Bus Data

Bus	Bus Type	Net Load [MW]
Ba-A0	Slack Bus	-
Ba-A1	PQ	-1000
Ba-B0	Slack Bus	-
Ba-B1	PQ	1200
Ba-B2	PQ	1300
Ba-B3	PQ	900
B0-C1	PQ	500
B0-C2	PQ	500
B0-D1	PQ	1000
B0-E1	PQ	100
B0-F1	PQ	500

Table 3. DCS1 Data

AC-DC Converter Station	Power Rating [MVA]	Operation Mode Set points
Cm-A1	800	Q = 0 VDC = 1pu
Cm-C1	800	AC Slack

Table 4. DCS2 Data

AC-DC Converter Station	Power Rating [MVA]	Operation Mode Set points
Cm-B2	800	Q = 0 VDC = 0.99pu
Cm-B3	1200	VAC = 1pu P = 800MW
Cm-E1	200	AC Slack
Cm-F1	800	AC Slack

Table 5. DCS3 Data

AC-DC Converter Station	Power Rating [MVA]	Operation Mode Set points	
Cb-A1	2*1200	VAC = 1pu	VDC = 1.01pu
Cb-B1	2*1200	VAC = 1pu	P = 1500MW
Cb-B2	2*1200	VAC = 1pu	P = 1700MW
Cb-C2	2*400	VAC = 1pu	P = - 600MW
Cb-D1	2*800	AC Slack	

Tables 3-5 introduce the data for all the AC-DC converter stations. Table 6 introduces the data for the DC-DC converter stations.

Table 6. DC-DC Converter Data

DC-DC Converter Station	Power Rating [MW]	Operation Mode Set points
Cd-B1	2000	P = 600MW
Cd-E1	1000	P = 300MW

Table 7-8 introduce the line data. All line lengths represented in Fig. 1 are given in km.

Table 7. DC Line Data

Line Data	R [Ω/km]	Max. current [A]
DC OHL +/- 400kV	0.0114	3500
DC OHL +/- 200kV	0.0133	3000
DC cable +/-400kV	0.011	2265
DC cable +/-200kV	0.011	1962

Table 8. AC Line Data

Line Data	R [Ω/km]	L [mH/km]	C [μF/km]	G [μS/km]	Max. current [A]
AC cable 145kV	0.0843	0.2526	0.1837	0.041	715
AC OHL 380kV	0.0200	0.8532	0.0135	-	3555

#### Acknowledgments

The authors gratefully acknowledge ANEEL (Brazilian Electricity Agency) and CTEEP (Sao Paulo State Power Transmission Company) for supporting the work.

**Authors:** prof. dr. Jose Antonio Jardini, Foundation for the Technological Development of the Engineering Sciences (FDTE), E-mail: [jose.jardini@gmail.com](mailto:jose.jardini@gmail.com); prof. dr. Thales Sousa, Federal University of ABC, E-mail: [thales.sousa@ufabc.edu.br](mailto:thales.sousa@ufabc.edu.br); msc. Marco Antonio Barbosa Horita, Foundation for the Technological Development of the Engineering Sciences (FDTE), E-mail: [marcoabh@gmail.com](mailto:marcoabh@gmail.com); msc. Marcos Bassini, Foundation for the Technological Development of the Engineering Sciences (FDTE), E-mail: [mtbassini@gmail.com](mailto:mtbassini@gmail.com); prof. dr. Ruben Romero, State University of Sao Paulo, E-mail: [ruben@dee.feis.unesp.br](mailto:ruben@dee.feis.unesp.br); prof. dr. Marcos Rider, State University of Sao Paulo, E-mail: [mjirider@dee.feis.unesp.br](mailto:mjirider@dee.feis.unesp.br); Marcos Rodolfo Cavalheiro, Sao Paulo State Power Transmission Company, E-mail: [mcavalheiro@ctEEP.com.br](mailto:mcavalheiro@ctEEP.com.br).

The correspondence address is:  
E-mail: [thales.sousa@ufabc.edu.br](mailto:thales.sousa@ufabc.edu.br)